Mechanisms of Mesothelioma Induction With Asbestos and Fibrous Glass [1]

Mearl F. Stanton *and* Constance Wrench, *Laboratory of Pathology, National Cancer Institute,*[2] *Bethesda, Maryland 20014*

SUMMARY—Three types of asbestos in 7 forms, 6 types of fibrous glass, 2 types of silica, and 2 types of metal particles were applied on a fibrous glass vehicle to the pleura of rats. In 2 years, amosite, chrysotile, and 4 different specimens of crocidolite yielded equally high incidences of pleural mesotheliomas in the range of 58–75%. Hand-milled crocidolite fibers not exposed to extraneous oils or metallic milling yielded dose-related tumor responses comparable to those of a standard reference milled crocidolite. Standard crocidolite, inducing a high incidence of mesotheliomas, caused fewer mesotheliomas (20–32%) when reduced to submicroscopic fibrils by excessive milling. Pulverized fragments of the steel mill and nickel metal at doses exceeding potential contaminating levels did not induce tumors. Microspheres of noncrystalline silica resulted in a single mesothelioma among 48 rats. The intact fibrous glass vehicle did not yield tumors, nor did its absence alter the incidence of crocidolite-induced tumors. However, when the fibrous glass vehicle and 2 other types of fibrous glass, ranging in mean diameters from 5–10 μ, were reduced to short fibrous fragments and applied to the pleura, 4 mesotheliomas were induced among 91 rats. Two forms of an especially fine fibrous glass, ranging from 0.06–3 μ in diameter, further milled to approach the length of asbestos fibers, resulted in moderately high incidences of mesotheliomas in the range of 12–18%. Thus carcinogenicity of asbestos and fibrous glass seems primarily related to the structural shape of these materials rather than to physicochemical properties.—J Nat Cancer Inst 48: 797–821, 1972.

MESOTHELIOMAS of the pleura and antecedent fibrous plaques, comparable to those resulting from asbestos exposure in man, can be induced readily in the rat and hamster by direct intrapleural application of asbestos (*1–8*). Such experiments attest to the carcinogenicity of asbestos and offer an excellent means of investigating those carcinogenic mechanisms involved.

Three years ago we began experiments based on initial investigations suggesting that quantitative data could be obtained if treated rats were observed for 2 years (*7*). Asbestos on gelatin-satu-

[1] Received November 8, 1971; accepted December 8, 1971.

[2] National Institutes of Health, Public Health Service, U.S. Department of Health, Education, and Welfare.

453-466—72——15

rated glass pledgets was applied directly to the pleura. The pledgets acted as a scaffoid to uniformly distribute and retain asbestos over a large area of the pleura, and, without asbestos, acted as an irritant that could serve as a control on the specificity of the carcinogenic response. The glass pledgets did not appear to be carcinogenic or to increase the incidence of asbestos-induced mesotheliomas. Therefore, we have continued to use them as a vehicle for convenience and accuracy. The results of 28 experiments designed to study factors related to the carcinogenicity of asbestos are reported.

MATERIALS AND METHODS

Twelve hundred weanling, penbred, pathogen-free, female Osborne-Mendel rats, a strain noted for hardiness and tolerance to surgical procedures, were housed 5 to a metal hanging-cage and fed conventional laboratory chow and water *ad libitum*. Test materials were implanted in the pleura when rats were between 11 and 16 weeks old, except for 2 groups treated between 42 and 47 weeks of age. Thin pledgets of autoclaved coarse fibrous glass measuring about 30 × 20 × 2 mm were trimmed to weigh 45 mg. The appropriate dose of test material was suspended in warm 10% gelatin and, during continuous agitation, 1.5 ml fractions were spread over the surface of each pledget. Control pledgets were treated with either gelatin alone or consisted of additional fibrous glass vehicle. All pledgets were allowed to harden at 4°C. The treated surface of a pledget was placed directly against the visceral pleura of the left lung through a 3-cm rib-spreading thoracotomy in rats anesthetized with open-drop ether. The incision was closed in layers to insure against leakage to subcutaneous sites. Postoperative mortality was <3%.

All groups were observed daily for 2 years. Only moribund rats were killed, and intrapleural neoplasms were detected only at necropsy. Survivors were killed during the 25th month after treatment. Detailed gross necropsy findings were recorded on 97% of the rats, and histologic sections from the implant site and all other grossly abnormal tissues were examined. Selected neoplasms were stained with periodic acid-Schiff, toluidine blue, mucicarmine, and Hale's for acid mucopolysaccharides, before and after digestion with diastase or hyaluronidase. Concurrently, 256 untreated rats were killed in groups of 50 at 6-month intervals during the 2½ years. These controls, like several thousand previously studied in this laboratory, had no primary intrathoracic neoplasms other than a rare thymic lymphoma and a distribution of neoplasms outside the chest essentially like that of the experimental groups. In our colonies, the average lifespan of this rat is less than 3 years; consequently, mortality from disease other than mesothelioma was high during the latter half of the experiment. Periodic epidemics of acute pneumonitis were controlled by oral tetracycline therapy; however, the partially compromised function of the treated left lung greatly increased mortality in rats with contralateral pneumonitis. During the 2d year of life, the mean incidence of mammary neoplasms in this strain is approximately 36%. Mammary tumors were surgically removed, histologic examination insuring that those of the left thorax did not represent invasion from underlying pleural neoplasms. Neoplasms of the adrenal cortex and genital organs are also common during the 2d year. Because these and other diseases represent a significant mortality factor, significant lesions and time of death were included in the text-figures.

Seventeen materials were applied to the pleura. Physical and chemical data on the asbestoses are detailed in (*9–12*); data on other materials were sparse. In each glass and asbestos sample, particles varied from submicroscopic to macroscopic dimension in both length and diameter. To obtain a simple estimate of size distribution, samples of the materials were suspended in water or Formvar, air-dried on glass slides, and photographed at 250 and 1000 magnifications (figs. 1–18). Similar preparations impressed on Formvar-coated copper grids were examined in an AEI-EM6B electron microscope.

Characterization of the test samples was obtained from information or analyses made in this laboratory or supplied by manufacturers and processors.[3]

Coarse coated fibrous glass vehicle.—The pledgets in all experiments were from a single source of flexible, thermal insulation, fibrous glass of the type used in building construction. They consisted of meshworks of long intertwining strands of borosilicate glass coated with a heat-cured, phenol-formaldehyde resin. In addition to silicon, they contained elements noted in table 1. The strand diameters were 3–10 times greater than the asbestoses, with a mean diameter of 5 μ and with a few fibers in both the <1 and >25 μ range (fig. 16).

UICC standard reference samples of asbestos (croicdolite, amosite, chrysotile A).—In 1964 the International Union Against Cancer, on the recommendation of a working group, established Standard Reference Asbestos Samples (SRAS) of the major types of asbestos prepared from as typical a parent material as possible (*9, 10*). Three of these samples, crocidolite, amosite, and chrysotile A were included. The UICC-SRAS crocidolite served as a base for comparative studies with the other materials. The samples, received in polythene plastic bags from Penarth, Wales, were stored in glass containers. All 3 samples have been characterized both physically and chemically (*11, 12*).

[3] We are indebted to Johns-Manville Research and Engineering Ctr., Manville, N.J.; Owens-Corning Fiberglas Corp., Toledo, Ohio; Corning Glass Works, Corning, N.Y.; Pneumoconiosis Research Unit, Llandough Hospital, Cardiff, Wales; National Bureau of Standards, U.S. Dept. of Commerce, Gaithersburg, Md., and the U.S. Bureau of Mines, U.S. Dept. of Interior, College Park, Md.

South African crocidolite (Wagner preparation).—Milled crocidolite from a single source of Northwest Cape Blue asbestos was obtained from Dr. J. C. Wagner. It was originally used to determine carcinogenicity in the rat by Wagner *et al.* (*1, 2, 5, 6*) and later by our laboratory (*7*). Physical and chemical properties have been documented (*13–15*).

UICC-SRAS crocidolite (partially pulverized).—To treat asbestos like some glass samples, the UICC-SRAS crocidolite was partially pulverized in a Spex model 5000 stainless-steel ball mill (Spex Industries, Inc., Metuchen, N.J.), operating at 3200 rpm for 1½ minutes, with 15 mg loads in 2-ml chambers. X-ray diffraction analysis of samples of this crocidolite after comparable pulverization was done by both the National Bureau of Standards and the Johns-Manville Research and Engineering Center. These analyses indicated a persistence in the diffraction lines characteristic of crocidolite, though areas beneath selected peaks were reduced. Electron microscopic examination indicated that the nonfibrous particles by optical standards were essentially clumps of submicroscopic fibrils (fig. 8); consequently, the changes in the X-ray diffraction pattern probably represented changes in fiber size, though loss in the crystalline structure of the asbestos fiber may also have occurred.

Virgin crocidolite ore, hand-milled.—A single hand-cobbed ore specimen measuring approximately 8 × 8 × 10 cm was obtained from Mr. L. N. Kuyper, of Cape Asbestos South Africa (Pty.) Ltd. Much of the stratified fibrous vein was separated from extraneous minerals by hand. Grinding by hand the halves of the ore surface reduced the separated fibers to fibrous dimensions roughly comparable to those of the UICC-SRAS crocidolite.

Virgin crocidolite ore, ball-milled.—Other portions of the stratified fibrous vein from the above ore sample were briefly fragmented in the Spex mill until reduced to a quality comparable to the UICC-SRAS crocidolite.

Spex stainless-steel mill fragments.—A stainless-steel chamber of the type used in our milling process was reduced to minute fragments with a carbide steel lathe, and these fragments were further pulverized for 30 minutes in the mill. Most particles ranged from 2.5–40 μ. This nickel-chrome steel was not analyzed for trace elements.

Metallic nickel fragments.—The nickel was purified precipitate from disintegration of nickel carbonyl, composed of 2- to 100-μ aggregates of particles that rarely exceeded 1 μ in diameter. By electron microscopy, these particles were covered with spiny projections. The sample, originally obtained from the International Nickel Company, Toronto, by Dr. W. C. Hueper, yielded sarcomas in the rat at a cumulative intrapleural dose of 300 mg (*16*).

Other glasses.—The coarse fibrous glass that served as a vehicle and 4 other types of fibrous glass were tested for carcinogenicity after they were reduced in the Spex mill to fiber lengths of 1–20 μ, roughly comparable to those of asbestos.

Figures 9–16 indicate the distribution of fiber sizes and particularly the quantity of the materials reduced to nonfibrous particles by milling, *i.e.*, particles with length-to-diameter ratios of less than 3:1. Although limited material could be examined with the electron microscope, fibers <0.5 μ in diameter were in all partially pulverized glasses and particularly abundant in the AAA fibrous glass. Table 1 indicates the chemical content of these glasses, exclusive of the major silicate component; other features before milling are given below.

Fibrous Pyrex glass wool.—A commercial product used in coarse filtration procedures consisted of long silky fiber 5–12 μ in diameter, coated with a binder of undetermined composition.

Old glass wool.—An obsolete loose commercial fiber, popular several decades ago as house insulation, consisted of abundant short fibers ranging from 1–35 μ in diameter, with many hook-ended fibers.

AAA fibrous glass.—Two forms of this glass were tested after partial pulverization to reduce fiber length: uncoated glass designated AAA-u and identical glass coated with a urea-formaldehyde resin designated AAA-c. The mean diameter of whole fibers was 0.22 μ, with a range of 0.06–3 μ. The chemical composition and size range of the 2 were essentially identical (table 1).

Silicon dioxide.—Two forms of especially fine, noncrystalline SiO_2 (silica soot and Cab-O-Sil), prepared by flame hydrolysis of silica tetrachloride, were 99.9% pure. A considerable difference in particle size was apparent between the 2 types of silica at the optical level (figs. 12, 15). At the submicroscopic level, these particles were composed of agglutinated clumps of minute spheres that ranged from 5–15 nm for silica soot and 50–150 nm for Cab-O-Sil.

TABLE 1.—Minor mineral oxide content (percent) of 4 glasses analyzed* by emission spectroscopy after ignition at 1000°F

	Al_2O_3	B_2O_3	CaO	MgO	Fe_2O_3	Na_2O	TiO_2
Coarse fibrous glass (vehicle)	4.0	8.0	6.4	3.1	0.36	14.0	0.06
Fibrous Pyrex glass	3.6	5.5	14.0	2.4	0.62	13.0	0.05
Old glass wool	8.5	—	32.0	9.5	0.80	0.55	0.60
AAA fine fibrous glass	11.0	7.2	17.0	5.4	0.60	1.0	0.46

*By personnel of the Johns-Manville Research and Engineering Ctr. and the Owens-Corning Fiberglas Corp.

RESULTS

Analysis of Tumor Yield

The results of 28 experiments, each with 30 rats, are shown in text-figures 1–7. The text-figures, arranged in identical format for comparing data, are sufficiently detailed to permit alternative methods of calculation. Since the earliest mesothelioma was observed 54 weeks after treatment, we considered only those rats that survived the 1st year after treatment as the effective number. Each figure heading contains the overall incidence of mesotheliomas in this effective number. Within each text-figure the space below the baseline represents rats dead during the 1st year. Above this line the solid area represents rats dead with mesothelioma, and the outlined area, rats dead from other causes. This information is tabulated by week at the base of each text-figure. The extent of pleural fibrosis at the implant site was assessed in all rats dying during the 2d year on a 1–4 scale, and the predominant value is indicated at the lower right. An alphabetic code indicates the major lesions in each rat at death. Each letter represents an organ system, with upper-case letters indicating neoplasms and lower-case letters representing other lesions, primarily of inflammation or degeneration: A, adrenal; B, bone; C, cutaneous tissues; D, muscle; E, pancreas; F, peritoneum; G, digestive tract; H, liver; I, EENT; J, nervous system; L, respiratory tract; M, mammary glands; O, genitalia; P, pituitary; Q, thymus; R, lymphoreticular system; S, spleen; T, thyroid; U, urinary system; V, vascular system; W, salivary glands; X, no lesions; Y, generalized disease; Z, lost or unaccounted.

Text-figures 1a–d compare the incidence of mesotheliomas after a maximum dose of 40 mg for 4 different types of asbestos. The first mesothelioma to kill a rat occurred in the amosite group during the 54th week. Two further lethal mesotheliomas were in this group before the 68th week, suggesting an earlier onset of neoplasms with amosite than with chrysotile or the crocidolites—a phenomenon also apparent in Wagner's experiments (*2*, *17*). However, during all comparable periods in the last three-quarters of the 2d year, the cumulative incidences of deaths with mesothelioma from the 4 types of asbestos were similar, and the final incidences of pleural neoplasms were not statistically different (15/25, 15/26, 14/23, 15/20). These high incidences suggest that 40 mg could have been in excess of the dose necessary to induce a maximum tumor response. However, this is unlikely, since half this dose of UICC-SRAS crocidolite yielded appreciably fewer mesotheliomas (text-fig. 2a). Fibrosis at the implant site was uniformly high in all 4 groups and served as a basis for comparisons to follow. One rare neoplasm, a generalized lymphosarcoma not involving the pleural site, was found in the chrysotile group.

Text-figures 2a–d illustrate the response with UICC-SRAS crocidolite in graded doses from 20–1 mg. With the data from text-figure 1c on the 40-mg dose, it was clear that a dose-response relationship existed both for the apparent time of tumor onset and for final incidence of pleural neoplasms. From these data, a dose of approximately 23 mg was calculated by graphic probit analysis to yield a 2-year 50% mesothelioma incidence if deaths from other causes remained constant (*18*). Fibrosis, less extensive than at 40 mg, occurred in all rats at doses of 10 and 20 mg, and lesser degrees of fibrosis occurred at lower doses. In these groups, 4 relatively rare neoplasms were noted: an osteogenic sarcoma of the skull, 2 hemangiomas of the spleen, and a peritoneal lipoma.

Text-figures 3a–c show 3 controls for the experiments with only pledgets of the large-diameters fibrous glass of the vehicle laden with gelatin. In the 3 experiments, none of the 90 rats had pleural neoplasms. However, only 58 rats survived the 1st year to serve as valid treated controls; thus incidences of mesotheliomas as hight as 3/30 rats in comparable experiments could conceivably result from the vehicle fibrous glass alone (*19*). Initial inflammatory reaction to the pledgets was as vigorous as to pledgets saturated with asbestos. But with time, far less fibrosis occurred than with doses of 1 mg crocidolite, and only minute residues of glass and scar tissue were detected in rats killed at the end of the experiments.

Text-figure 3d represents the control experiment to determine the effect of the glass pledget on neoplasms induced with asbestos. A median dose of 10 mg UICC-SRAS crocidolite was suspended in physiologic saline and delivered to the left pleura through an open thoracotomy without the

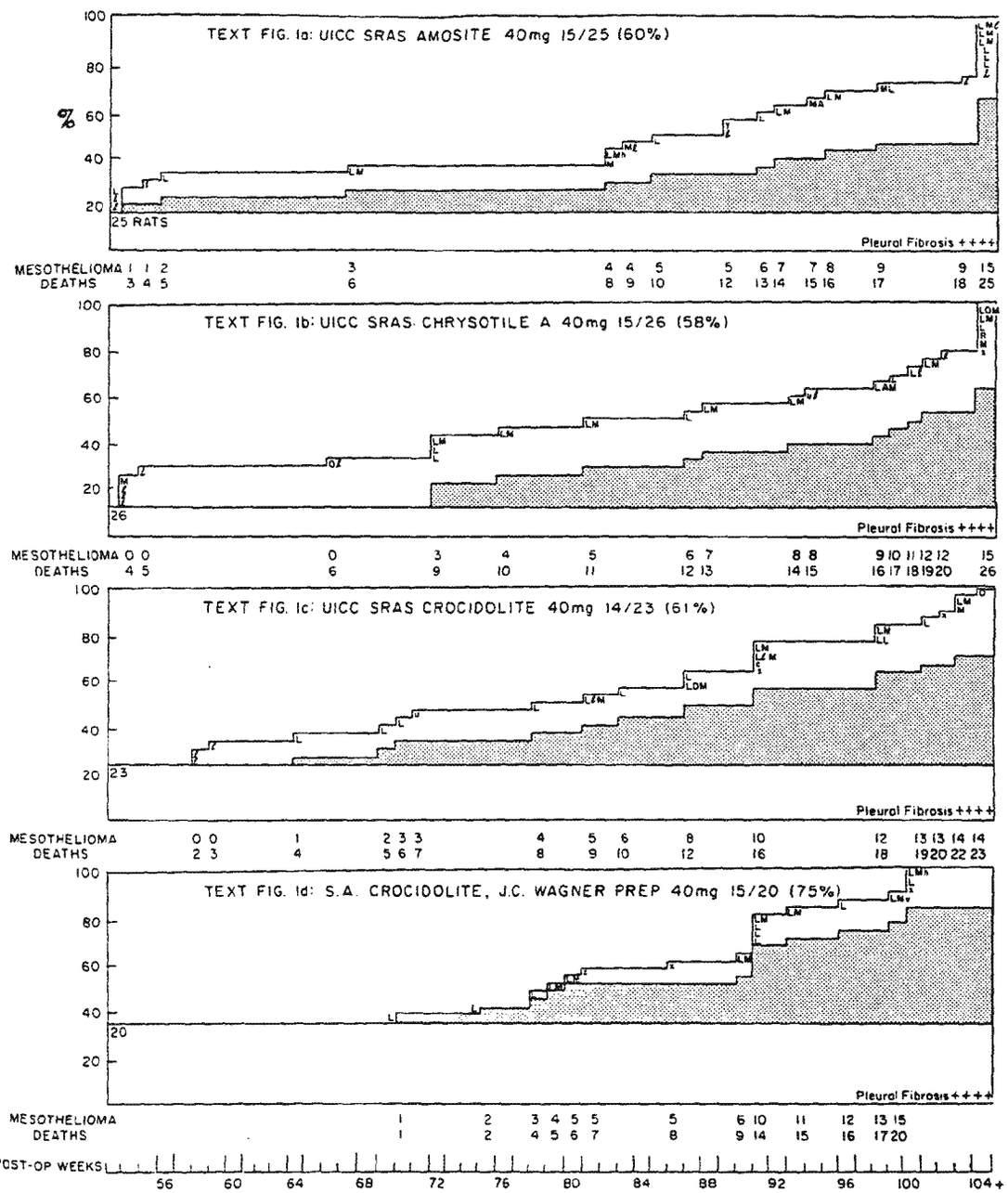

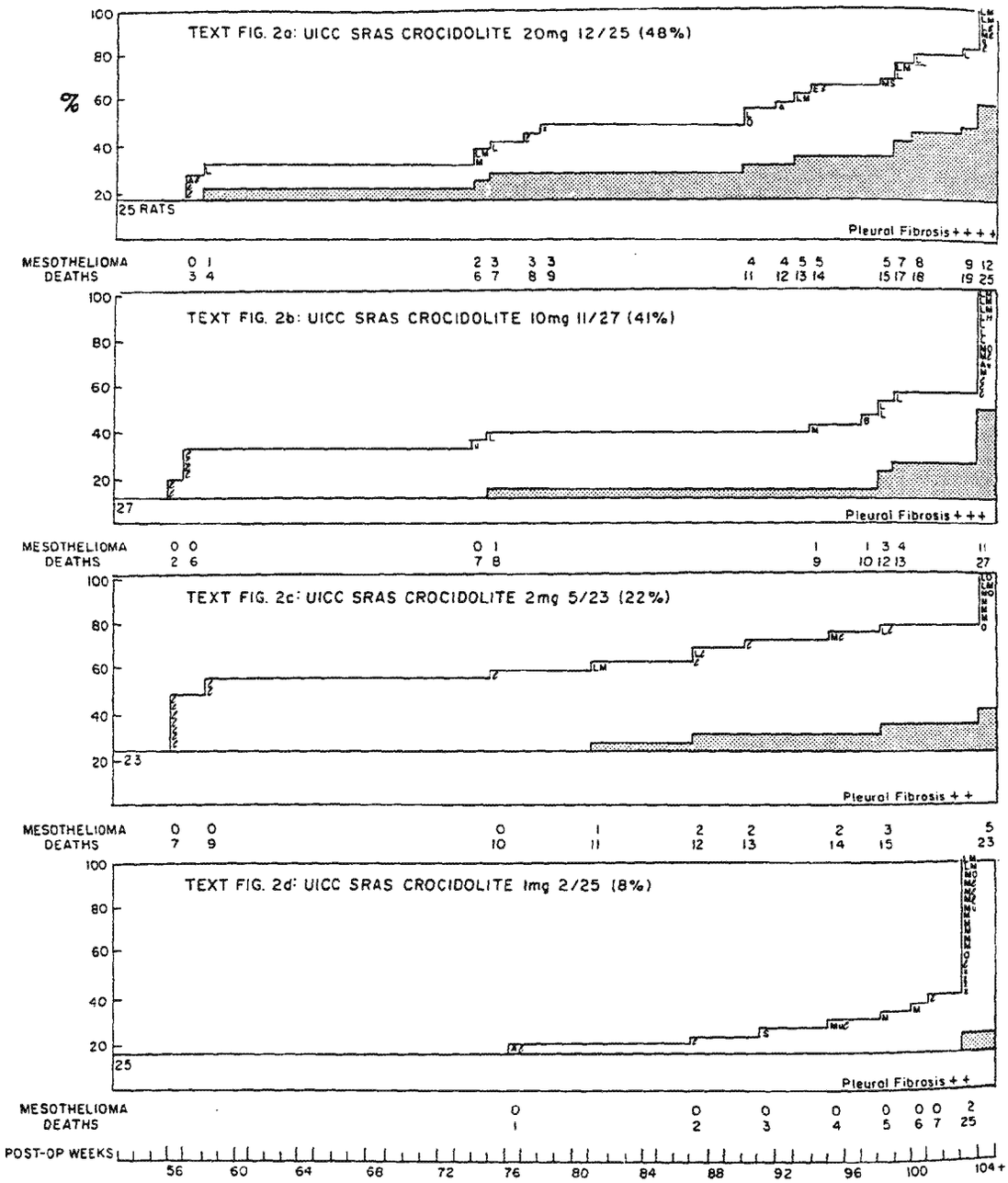

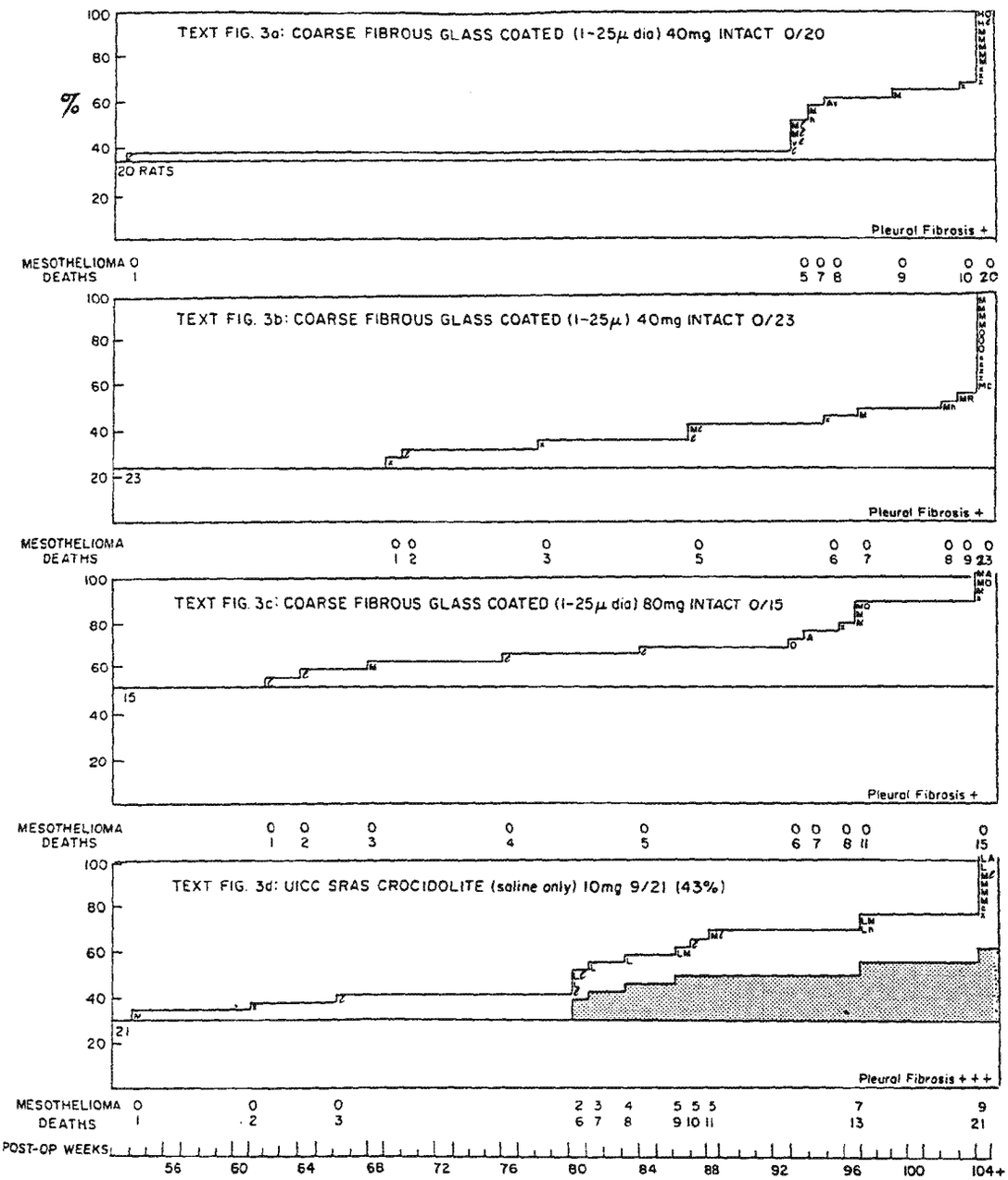

glass vehicle. We expected fewer tumors because asbestos injected in this manner tended to pool in the costophrenic angle. However, when this result is compared with that of an identical dose on glass pledgets (text-fig. 2b), the final incidence in the 2 experiments (9/21 vs. 11/27) indicates that the glass neither enhanced nor suppressed the induction of mesotheliomas by asbestos.

Text-figures 4a–c present results after application of crocidolite from a single specimen of Northwest Cape crocidolite ore hand-milled in our laboratory, with only the fiber block as a milling medium. The incidence of mesotheliomas at levels of 40 and 20 mg was virtually identical to that of the UICC-SRAS crocidolite, and at the 1-mg level no significant difference in response was evident (2/25 vs. 4/30) ($P>0.5$). A graphic probit analysis of dose response over this range indicated that a 25-mg dose would yield a 2-year 50% mesothelioma incidence compared with the 23-mg 50% tumor dose for UICC-SRAS crocidolite (*18*). The extent of pleural fibrosis correlated with dose and closely matched that of comparable doses of the UICC-SRAS crocidolite. Text-figure 4d illustrates the result of 40 mg of the same crocidolite fiber block after milling in a stainless-steel ball mill. Here again the 15/23 incidence of pleural neoplasms was virtually identical with the 14/23 incidence from UICC-SRAS crocidolite (text-fig. 1c) and with the 18/27 incidence from the hand-milled crocidolite (text-fig. 4a). Both implant site fibrosis and extrathoracic tumor incidence followed that of the 2 previous crocidolite tests. Indications that mill contamination was not a factor in asbestos carcinogenesis were further supported by the experiments shown in text-figure 5.

The experiments in text-figures 5a and b explore the carcinogenic potential of nickel-chrome steel, the prime metallic contaminant in the milling process, and of nickel, a known carcinogenic constituent of the mill. Pulverized particles of nickel-chrome steel from a mill like the one used to process the crocidolite ore yielded no mesotheliomas at a dose equal to that of the highest level of asbestos. Pure nickel at similar high levels was excessively toxic; all rats were dead with hemorrhagic pneumonitis within 60 days. Consequently, we used a 1-mg dose, still far in excess of potential nickel contamination from the mill. Toxicity of the nickel, even at this level, was high in the 1st year, but no pleural neoplasms developed in 18 rats having a survival rate during the 2d year comparable to that of the asbestos-treated groups. The experiments in text-figures 5c and d concern the carcinogenic potential of silica, the predominant constituent of both asbestos and glass. Silicon dioxide was used in the form of amorphous (*i.e.*, noncrystalline), smooth-surfaced spheres of submicroscopic size. In these 2 experiments, a single mesothelioma developed early in the 2d year. All 4 experiments with nonfibrous materials produced a minimum of pleural fibrosis, though the degree of fibrosis seemed greater with the steel fragments than with the other materials. In the nickel-treated group, 2 rare tumors, a pituitary adenoma and a carcinoma of the kidney, were noted.

Text-figures 6a and b represent our first attempts to examine nonasbestiform fibers of a size similar to asbestos. The glass with large fiber diameters that was used as a vehicle was reduced to fibers 1–20 μ long by milling in a stainless-steel ball mill, applied to the glass vehicle, and implanted in 2 groups of rats. In the first group, the rats were young as in the other experiments, but in the second group, 40-week-old rats were used to test age-related susceptibility. Two further experiments (text-figs. 6c, d) were done on fibrous glasses of slightly smaller diameters reduced to lengths of 1–20 μ: the highly irritating old glass wool and Pyrex fibrous glass. The results of all 4 experiments were essentially alike in that only single pleural neoplasms occurred in each experiment, the degree of pleural fibrosis was minimal, and unusual neoplasms were rare. Although no mesotheliomas had been noted with the intact fibrous glass vehicle, 4 mesotheliomas indicated that fibrous glass could be carcinogenic if reduced to fibrous lengths of 1–20 μ. However, the low incidence of mesotheliomas (4/91) and the low number of negative controls were insufficient to show that partially pulverized glass was potentially more carcinogenic than the intact glass.

Text-figures 7a and b show 2 experiments done in the same way with fibrous glass of much finer diameter than the glasses with coarse fibers. The 2 samples were identical except for a coating of

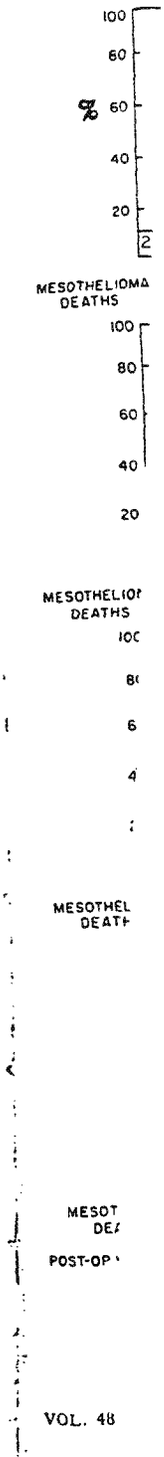

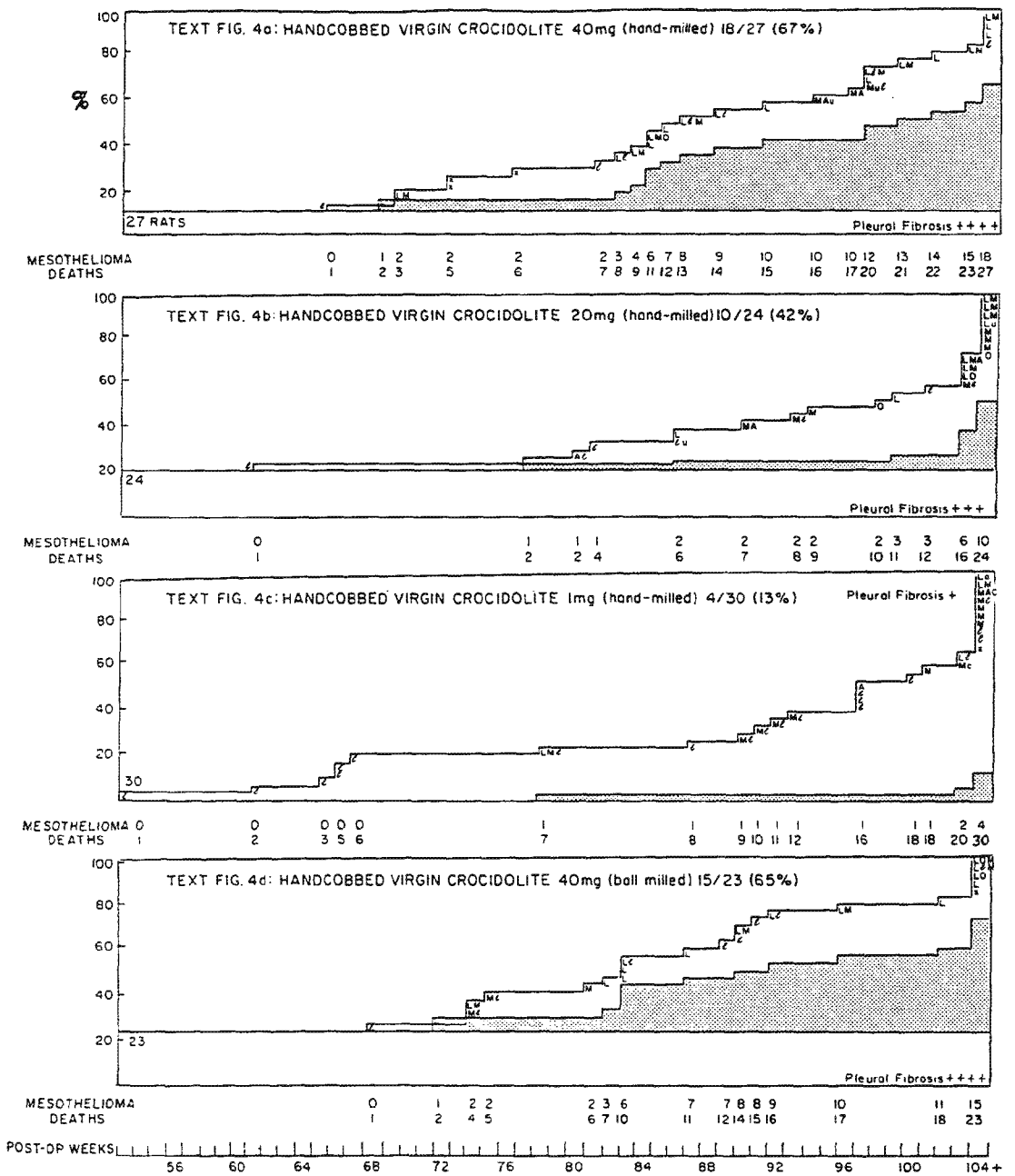

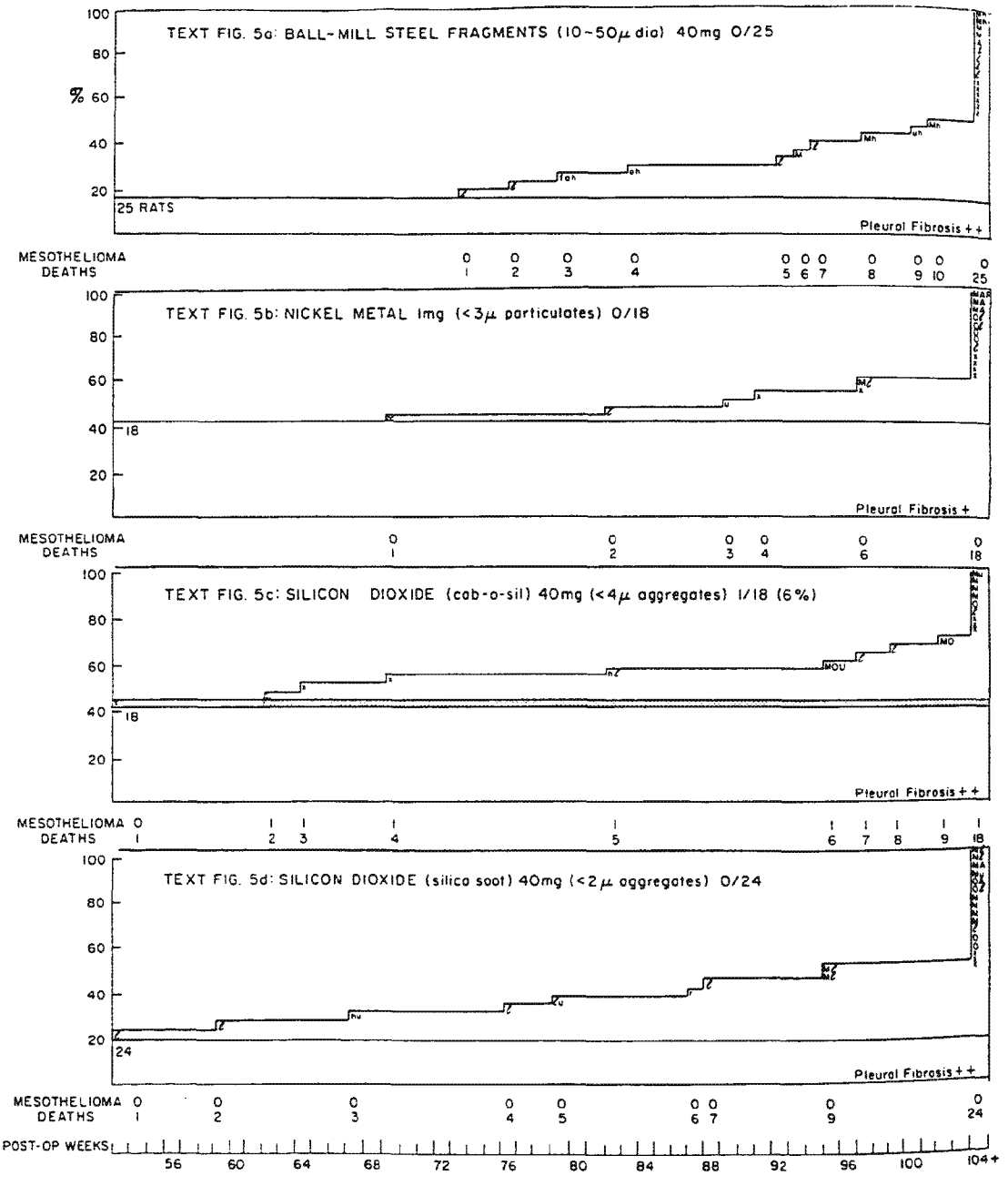
TEXT FIG. 5a: BALL-MILL STEEL FRAGMENTS (10-50μ dia) 40mg 0/25
25 RATS
Pleural Fibrosis + +
MESOTHELIOMA DEATHS
TEXT FIG. 5b: NICKEL METAL 1mg (<3μ particulates) 0/18
18
Pleural Fibrosis +
TEXT FIG. 5c: SILICON DIOXIDE (cab-o-sil) 40mg (<4μ aggregates) 1/18 (6%)
Pleural Fibrosis + +
TEXT FIG. 5d: SILICON DIOXIDE (silica soot) 40mg (<2μ aggregates) 0/24
24
POST-OP WEEKS
56 60 64 68 72 76 80 84 88 92 96 100 104+

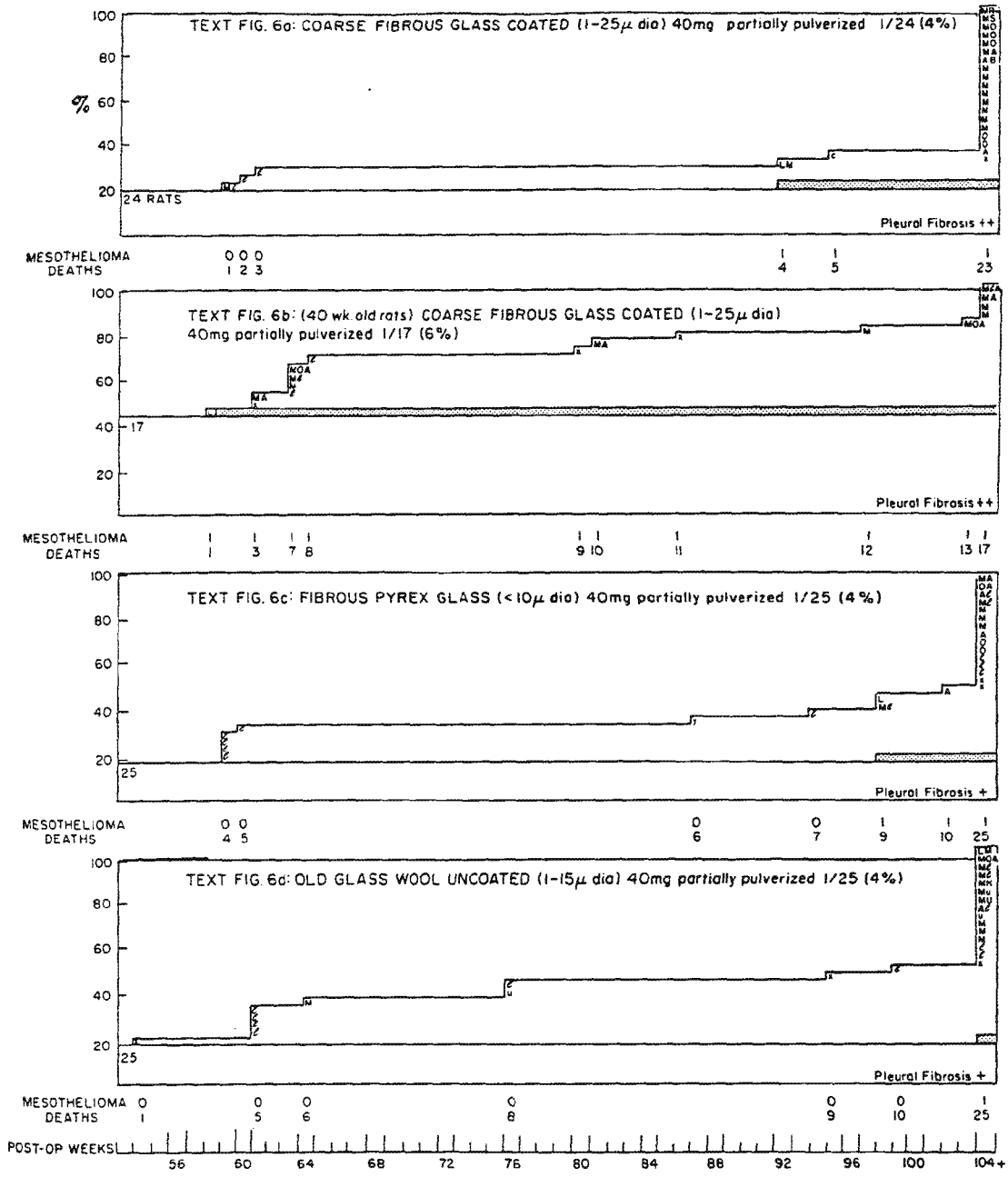

urea-formaldehyde resin on the second. The partially pulverized fibers had mean lengths of about 5 μ and diameters ranging from 0.06–3 μ, resembling the range of medium-sized asbestos fibers. Each experiment showed a small but significant number of mesotheliomas, 3/26 and 5/28. These data taken together indicate a statistically significant increase in incidence over the experiments with intact coarse-glass vehicle (8/54 vs. 0/58) ($P<0.05$) and the combined experiments with partially pulverized glass of larger diameter (8/54 vs. 4/91) ($P<0.05$). Pleural fibrosis was greater also in these groups than those treated with fibrous glass of larger diameter.

Text-figures 7c and d represent experiments originally designed as controls on the experiments with partially pulverized glass. Groups of both young and old rats were implanted with UICC-SRAS crocidolite that had been further pulverized in our ball mill for 1½ minutes. Gross effects of the additional milling were not apparent, but subsequent microscopic examination indicated appreciable reduction in particle size (figs. 7, 8). In both experiments the number of mesotheliomas and the extent of pleural fibrosis decreased as compared with the 4 groups treated with unpulverized crocidolite. Since this difference seemed particularly important, a cumulative mortality rate for mesotheliomas corrected for extraneous deaths was plotted by the method of Pilgrim and Dowd (*20*). Text-figure 8 indicates the consistently high mesothelioma incidence for the 4 groups treated with nonpulverized crocidolite and the consistent reduction in mesothelioma incidence throughout the 2 experiments with partially pulverized crocidolite. A chi-square test comparing the incidence of mesotheliomas between the single group of young rats treated with partially pulverized crocidolite (text-fig. 7c) and each of the 4 comparable age groups treated with nonpulverized crocidolite (text-figs. 1c, 1d, 4a, 4d) indicated a probability of a valid difference of 95% when calculated for 2 of the 4 groups and more than 99% for the other 2 groups, or for the 4 groups combined.

Fiber Size in Relation to Tumor Yield

Results pointing to differences in tumor response relevant to particle size motivated an assessment of the size distribution of fibers of the 17 materials. The wide range in dimensions in each of the 17 materials made precise tabulation of the size of individual particles formidable. Consequently, we assigned 1000 consecutively counted particles to 30 ranges of dimension to give us a fair sampling of size distribution in the optical range (table 2, part A). The preparations counted are illustrated at low magnification in figures 1–18. Extending these ranges to particles of submicroscopic size proved futile because of the limited sample size that could be evaluated by electron microscopy. However, our impressions were as follows: In all asbestos and glass samples, fibers (*i.e.*, particles with ratios of diameter to length of 1:3 or greater) extended nearly to the limits of electron microscopic resolution. Fibers less than 1.0 μ in diameter were far more numerous in asbestos samples than in glass samples. Large and small clumps of asbestos that appeared nonfibrous in the optical range were composed of clumps of microfibrils in the range of 0.05–0.2 μ × 0.6–2.0 μ (fig. 8). In contrast, nonfibrous glass particles were irregular, solid masses. Neither the silica nor metal samples contained fibrous particles. Nickel particles were irregular, sharply angulated, spiny crystals; both types of silica were smooth-surfaced spheres.

Since dose was determined by weight, we further estimated the number of particles in each dimensional range per unit weight by considering density. Part B of table 2 represents this estimate, assuming that the particles were cylinders and that the particles in each dimensional range were distributed uniformly about the mean volume for each range. In the ranges with few large fibers, these assumptions were liable to error. Furthermore, the whole fibrous glass used as a vehicle could not be treated this way, since the length of most fibers exceeded limits that could be measured accurately. Despite this defect in methodology, we believed that such estimates might be revealing if only broad differences in carcinogenic response and particle distribution were compared.

Considered in this way, 3 of the 4 conventionally milled crocidolite preparations with equally high tumor response had similar distributions of particles. The one deviation was UICC-SRAS crocidolite, which had few fibers in excess of 5 μ in diameter and a consequent abundance of finer

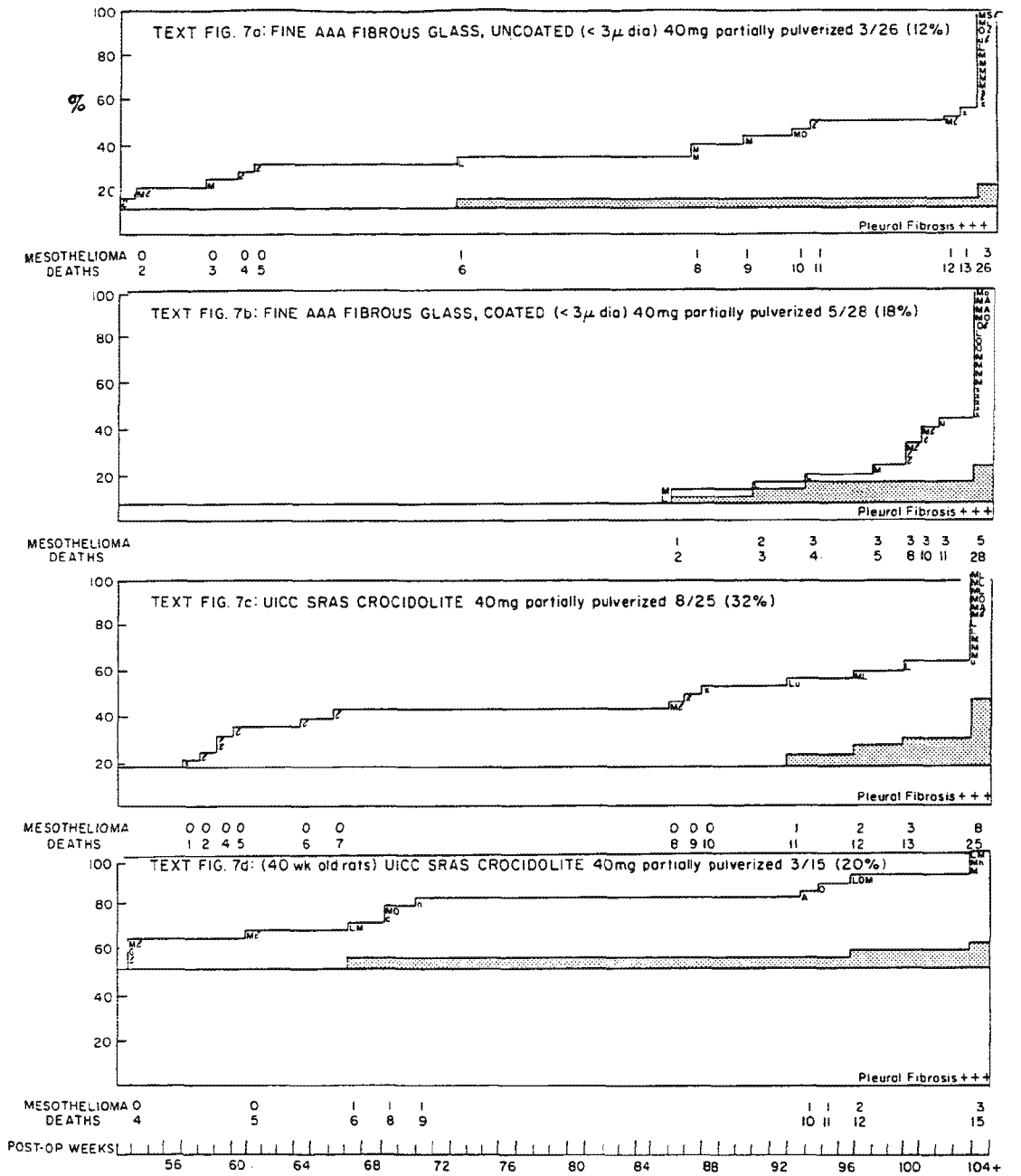

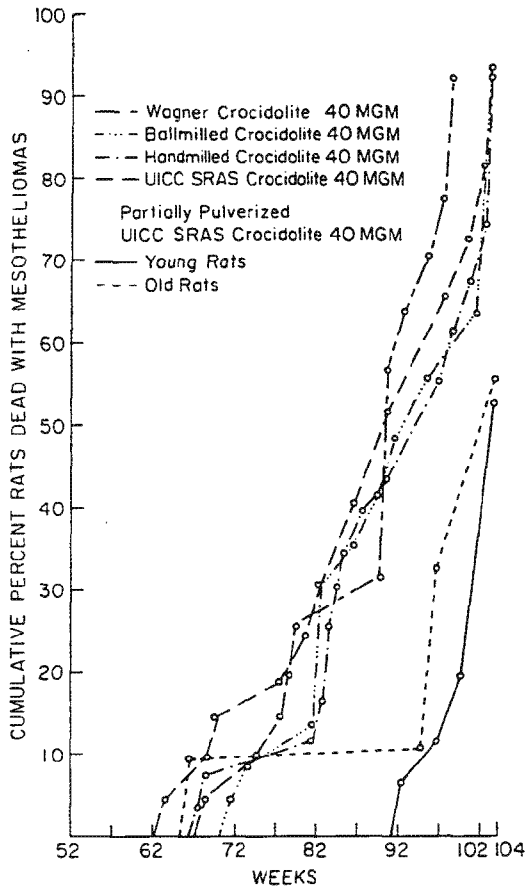

TEXT-FIGURE 8-CUMULATIVE TUMOR MORTALITY CORRECTED FOR EXTRANEOUS DEATHS

fibers because of more complete milling. Similarly, the UICC-SRAS amosite and chrysotile preparations with comparably high tumor responses contained few large fibers. From these data we could conclude either that fibrous particles exceeding 5 μ in diameter were not essential to the induction of tumors or that the large fibers were reduced to finer fibers *in vivo*.

The critical comparison was between the excessively milled, partially pulverized crocidolite with low tumor incidences and the conventionally milled crocidolites with high tumor incidences. Prolonged milling pulverized the crocidolite until no particles were greater than 2.5 μ in diameter or 20 μ long (table 2, part B). Over half the sample by weight (84% of the number of particles) consisted of minute clumps, not exceeding 2.5 μ in either dimension, that were nonfibrous by optical standards. However, these clumps, like those occurring less frequently in other asbestos samples, were composed largely of submicroscopic fibrils (figs. 7, 8). Since the number of these clumps of submicroscopic fibrils far exceeded those in the conventionally milled crocidolite samples, it was reasonable to assume that they were responsible for the loss in carcinogenicity. Presumably, the 20–32% tumor incidences resulting from this sample were related to those particles that retained their fibrous structure in the optical range. However, the 3 categories of optically apparent fibers represented in this low-tumor-yield sample each contained more fibers than their counterparts in samples that yielded high incidences of tumors. Furthermore, if one totaled all optically visible fibers in the low-tumor-yield, partially pulverized crocidolite, they numbered more than the totaled fibers in the high-tumor-yield crocidolites (table 2). Thus the incidence of mesotheliomas did not relate directly to either the number of fibers in a particular dimensional range or to the total number of fibers implanted. However, asbestos fibers are composed of bundles of microfibers which readily separate through fragmentation. Touch preparations from the lesions showed that fragmentation of both glass and asbestos occurred *in vivo*. Therefore, it seemed reasonable to consider the number of fibers present in the lesion if submicroscopic fibrils were discounted and all other fibers were reduced to a common dimension slightly greater than this size. The smallest fibers countable by light microscopy were in the mean range of 1.25 X 3.75 μ; these were designated microfibers. Converting all larger fibers to this dimension and excluding particles of lesser dimension yielded between 5584–7854 microfibers/0.1 μg for the 6 high-tumor-incidence, conventionally milled, asbestos samples (table 2, bottom line), while the low-tumor-incidence, partially pulverized, crocidolite sample yielded 3147 microfibers/0.1 μg—about half the microfibers of the high-tumor-incidence groups. By the same reasoning we considered the glass. We assumed that glass could fragment transversely as easily as asbestos, but since glass is not composed of microfibril bundles, longitudinal fragmentation would be rare. Conse-

quently, only transverse fragmentation of the glass fibers to lengths of 3.75 μ was calculated. For the 2 fine-glass samples inducing 12–18% mesotheliomas, the total number of calculated microfibers was 1127–1629/0.1 μg—half that of the partially pulverized crocidolite and less than one-fourth the conventionally milled asbestoses. The 3 coarse fibrous glass samples that yielded rare mesotheliomas had calculated numbers of 207–312 microfibers/0.1 μg—less than 20% those in the fine-glass samples and less than 5% those in the high-tumor-incidence asbestos samples. Thus mesothelioma incidence correlated reasonably well with the theoretical number of microfibers present in the lesions, irrespective of whether the material was glass or asbestos.

Morphologic Observations

The primary response of the pleura to asbestos implants was a vigorous granulomatous reaction resulting in dense fibrous coats firmly adherent to the visceral pleura and pericardium. This fibrous tissue, closely investing residual particulate matter, was composed of avascular, interlacing, immature spindle cells and abundant collagen interspersed with foci of hyalin and liquefactive necrosis (figs. 19, 20). Pleural fibrosis in each rat was assessed, grossly and histologically, as extensive, moderate, or slight. This simple evaluation indicated that the extent of fibrosis roughly correlated with the incidence of pleural neoplasms, not only in the high- and low-tumor-incidence groups but also in the medium-tumor-incidence groups treated with low doses of asbestos or fine-pulverized glass. One purpose of the glass as a control was to determine whether pleural cell proliferation in the milieu of an inflammatory effusion might act as an *in vivo* cell culture with a high potential for neoplastic transformation. Ideally, one would expect such a control to yield a reactive fibrosis as extensive as that of the asbestos; however, this was not the case. In all experiments yielding few or no mesotheliomas, irrespective of the material used, fibrosis was negligible. Reactive sites in these groups had abundant mononuclear leukocytes, foreign body giant cells, and capillary vessels, but a paucity of collagen and connective tissue (fig. 21). The dense, fibrous plaques, which characterized the primary reaction to asbestos and fine-pulverized glass, had many qualities of neoplasia (fig. 20), but neoplastic development was distinguished by abrupt conversion of the collagenous, connective tissue to masses of closely packed, atypical, disoriented cells extending beyond the residual foreign particulates and the reactive fibrosis. Abundant mitoses implied a rapidly lethal course. However, a large proportion of the neoplasms were in rats killed at the end of the experiments. These neoplasms were no different from those in rats dying earlier. Only 13% of the neoplasms metastasized or invaded adjacent structures (table 3). Therefore, most of these neoplasms were probably slow growing and confined to local sites for long periods. Significantly, a similar slow course often characterizes the mesotheliomas of man (*21*, *22*). The mesotheliomas had histologic characteristics like those previously described (*2*, *7*). The predominant cells were either spindle shaped or pleomorphic, sometimes intermixed as commonly seen in nonepithelial neoplasms of the rat. Some tumors contained giant multinucleate cells, others had osteogenic foci, and a few had tubulopapillary patterns suggesting surface-covering features of mesothelium (figs. 22–26). Efforts to identify hyaluronic acid were equivocal, though some contained neutral and acid mucopolysaccharides. The 14 neoplasms with foci of osteogenesis seem unique to our strain of rats. No differences were apparent between tumors induced by asbestos and glass. The single tumor induced by silica was the most common fibrogenic spindle-cell type.

DISCUSSION

Direct application of our results to the problems in man would be unwise because the method of application and the high doses used are remote from the usual exposure of man to fibers, but how these materials exert their carcinogenic effect is a critical problem, and current data seem adequate to develop a working hypothesis.

The present studies show that conventionally milled asbestoses of 3 types have a high intrinsic capacity for inducing neoplasms and that this capacity is virtually equal, regardless of the type of asbestos or its source. Furthermore, fibrous

TABLE 2.—Seventeen implanted materials distributed into particle size ranges and ranked by overall pleural neoplasm incidence

A.—Distribution of 1000 consecutively counted particles visible at 1000×

Overall Incidence of pleural neoplasms (percent)		75	67	65	61	60	58	20 32	18	12	4-6	6	4	4	0	0	0	0
Particle dimensions (μ), diameter × length		J.C. WAGNER croc.	Hand-milled croc. ore	Ball-milled croc. ore	UICC-SRAS croc.	UICC-SRAS amosite	UICC-SRAS chrys.	Part. pulv. UICC-croc.	Part. pulv. AAA-C glass	Part. pulv. AAA-U glass	Part. pulv. coarse glass	Cab-O-Sil SiO_2	Part. pulv. Pyrex glass	Part. pulv. glass wool	Silica soot SiO_2	Whole coarse glass*	Nickel metal frag-ments	Steel mill frag-ments
>1-2.5	>1-2.5†	640	559	598	442	363	466	849	394	291	330	86	120	346	949		187	126
"	>2.5-5	219	87	126	272	339	280	103	276	263	43		4	41				
"	>5-10	80	138	89	169	165	135	45	144	189	18			30				
"	>10-20	20	63	57	55	69	54	12	58	64	26			31				
"	>20-40	5	34	20	26	31	40		21	40	19			13				
"	>40-80	4	20	18	8	11	8		8	10	24					16		
"	>80-160	1	15	8	1	3	3		14	4	12			2		16		
"	>160-320	3	2		3	3	1		2	6	15					344*		
>2.5-5	>2.5-5†	6	48	58	6	8	9		26	56	105	593	465	287	21		286	144
"	>5-10	4				1			16	32	15			10				
"	>10-20	3	1		2	1			8	8	2			45				
"	>20-40	3	1		2	2	1		8	16	21			22				
"	>40-80				1				3	6	16			3		8		
"	>80-160	1	3		3				3	2	23							
"	>160-320		2	1	1	1				2	30			2		288*		
>5-10	>5-10†	5	16	16	1	3	3		6	1	41	138	225	110	15		361	373
"	>10-20								2	2	19		36					
"	>20-40												51	13				
"	>40-80				1				4	4	5		38	3				
"	>80-160				1				4	4	11		7					
"	>160-320	1		3					3		74					232*		
>10-20	>10-20†	1	8	3							35	149	45	37	12		146	150
"	>20-40												7					27
"	>40-80													2				
"	>80-160										5			3				
"	>160-320	1		1							20					64*		
>20-40	>20-40†	2	3	2							1	34	2		3		20	167
"	>40-80																	43
"	>80-160																	
"	>160-320															32*		

B.—Estimated number of particles in each size range/0.1 μg†

B. Estimated number of particles in each size range/0.1 μg†

>1–2.5	>1–2.5†	181	157	133	578	896	2135	10,966	188	183	6.6	3.0	9.6	58	420	2.3	0.3
"	>2.5–5	62	25	28	356	837	1283	1345	131	166	0.9		0.3	6.9			
"	>5–10	23	39	20	221	407	618	588	69	119	0.4			5.0			
"	>10–20	5.7	18	13	72	170	247	167	28	40	0.5			5.2			
"	>20–40	1.4	9.6	4.4	34	77	183		10	25	0.4			2.2			
"	>40–80	1.1	5.6	4.0	11	27	37		3.8	6.3	0.5						
"	>80–160	0.3	4.2	1.8	1.3	7.4	14		6.7	2.5	0.2			0.3			
"	>160–320	0.8	0.6		3.9	7.4	4.6		1.0	3.8	0.3						
>2.5–5	>2.5–5†	1.7	14	13	7.9	20	41		12	35	3.9	23	37	48	9.3	3.4	0.3
"	>5–10	1.1				2.5			7.6	20	0.3			1.7			
"	>10–20	0.8	0.3		2.6	2.5			3.8	5.9	0.1			7.5			
"	>20–40	0.8	0.3		2.6	4.9	4.6		3.8	10	0.4			3.7			
"	>40–80				1.3				1.4	3.8	0.3			0.5			
"	>80–160	0.3	0.8		3.9				1.4	1.3	0.5						
"	>160–320		0.6	0.2	1.3	2.5				1.3	0.6			0.3			
>5–10	>5–10†	1.4	4.5	3.6	1.3	7.4	14		2.9	0.6	0.8	5.3	18	18	6.6	4.3	0.9
"	>10–20								1.0	1.3	0.4		2.9				
"	>20–40												4.1	2.2			
"	>40–80				1.3				1.9	2.5	0.1		3.0	0.5			
"	>80–160				1.3				1.9	2.5	0.2		0.6				
"	>160–320	0.3		0.7					1.4		1.5						
>10–20	>10–20†	0.6	2.3	0.7							0.7	5.7	3.6	6.2	5.3	1.7	0.4
"	>20–40												0.6				0.1
"	>40–80													0.3			
"	>80–160										0.1			0.5			
"	>160–320	0.3		0.2							0.4						
>20–40	>20–40†	0.6	0.8	0.4							0.1	1.3	0.2		1.3	0.2	0.4
"	>40–80																0.1
"	>80–160																
"	>160–320																
Total fibrous particles/0.1 μg		98	103	72	713	1546	2391	2089	273	411	8	0	12	37	6	0	1
Total nonfibrous particles/0.1 μg		186	178	151	588	924	2190	10,966	203	219	12	38	69	131	443	12	2
Estimated microfibers averaging 3.75 μ long/0.1 μg§		6189	5584	5863	6099	6278	7854	3147	1127	1679	249	0	207	312	0	0	11

*Most particles exceeded lengths of 320 μ.

†Nonfibrous compartments (nonfibrous asbestos particles most often represent mixtures of nonasbestiform minerals and clumps of submicroscopic fibrils).

‡ $P = \frac{np}{vd}(10^8)$ where np = number of particles counted in a given size range;
v = total volume of the 1000 particles counted in μ^3, assuming that the particles are cylinders and in each size range have volumes of a normal distribution; d = density.

§Assuming that all fibers fragment *in vivo* to mean lengths of 3.75 μ and that all asbestos fibers fragment longitudinally to mean diameters of 1.25 μ.

TABLE 3.—Histologic types of 169 mesotheliomas induced by asbestos and glass

Mesotheliomas	Asbestos	Glass
Spindle-cell types:		
Fibrogenic	105 (13)*	9 (1)
Osteogenic	12	2 (1)
Giant cell	9 (2)	
Pleomorphic cell types:		
Medullary	23 (3)	1
Tubulopapillary	8 (2)	
Total	157 (20)	12 (2)

*Figures in parentheses are the number of neoplasms that metastasized or invaded structures outside the thorax.

glass, when reduced to a distribution of sizes approaching that of conventionally milled asbestos, is also carcinogenic. This capacity to induce neoplasms might be related to 1) contamination by carcinogenic hydrocarbons and metals, 2) the carcinogenic constituents of the fibrous mineral itself, or 3) the structural character of the fiber.

Natural contaminating oils and minerals and those introduced in the milling and packaging of asbestos have been thoroughly investigated as causes of asbestos carcinogenicity (*2, 6, 14, 23–25*). Asbestos from which oils have been rigorously extracted is as carcinogenic as the nonextracted asbestos, and the contaminating hydrocarbons are not present in amounts sufficient to account for asbestos carcinogenicity. Experiments reported here concern the effect of contaminating metals—a hypothesis suggested by the findings of other investigators (*13, 14, 16, 26, 27*). Such metals have carcinogenic potential but seem unlikely causes of asbestos carcinogenicity because of the minute amounts involved. Our experiments show that, at levels far exceeding those that might contaminate asbestos, neither finely particulate nickel nor nickel-chrome steel is sufficiently carcinogenic to account for the mesotheliomas induced in the rat with asbestos. This observation would not exclude a synergistic or catalytic action of contaminating metals. But such a hypothesis is not supported by the experiments which show that hand-cobbed crocidolite fibers, milled without exposure to metal, induce numbers of mesotheliomas at graded dose levels equal to those of the same sample ground in a steel ball-mill or machine-milled UICC-SRAS crocidolite.

These experiments would not exclude the possible carcinogenicity of the variety of heavy metals or other complex constituents of the asbestos fiber itself. But great differences in the composition of different types of asbestos do not alter the carcinogenicity of the asbestos fiber as indicated in these and other experiments (*2, 3, 6, 12, 13*). Silicon dioxide, a major constituent of both asbestos and glass, proved relatively inert in our experiments. The single tumor in 48 rats may have been the result of the fibrous glass vehicle.[4] Further evidence against the idea that the chemical constituents of the fiber cause the neoplasms is the result with partially pulverized crocidolite. Prolonged milling not only reduced the fibers to clumps of submicroscopic fibrils but also exposed this residue to additional metal contamination from the mill. The resultant loss in carcinogenicity implies that the structural integrity of the asbestos fiber above that of the finest submicroscopic fibril is essential to carcinogenicity, and that neither contaminants nor chemical components are likely factors.

If this is so, then similar fibers, if sufficiently durable, should induce similar tumors. In our experiments, we reduced 3 types of coarse fiber glass to a range of sizes that spanned the range of asbestos, and this glass yielded a few mesotheliomas, even though it had far more large fibers and few of the minute fibers so abundant in asbestos. Experiments with the partially fragmented AAA glass of especially fine diameter further supported the critical importance of fiber size, for here, where the range in fiber sizes more closely matched that of asbestos, a relatively high incidence of meso-

[4] This negative result must be reconciled with the high incidence of intrathoracic reticulum cell sarcomas induced with an "alkaline-washed, silica sand" by Wagner *et al.* (*2, 4, 6*). They emphasized that silica-induced tumors were unlike those caused by asbestos and perhaps resulted from a different mode of induction. The absence of such neoplasms in our experiments may be related to differences in the physical structure of the silicas used by us and Wagner. Because we were interested in testing simply silicon dioxide, we used material prepared by flame hydrolysis. These silicas were exceptionally pure and composed of clumps of particles 5–150 nm in diameter that were spherical and noncrystalline. Neither type caused the extensive reactive fibrosis characteristic of freshly fractured crystalline quartz silica—a biological response that may be relevant to carcinogenesis (*28*).

theliomas was obtained. Furthermore, assuming that larger fibers tended to be reduced *in vivo* to a narrow range of sizes just above the limit of optical resolution, we could correlate the number of these microfibers potentially present in the lesions with the incidence of mesotheliomas, irrespective of the type of asbestos or glass.

All our experiments require extension, but the simplest incriminating feature for both carcinogenesis and fibrogenesis seems to be a durable fibrous shape, perhaps in a narrow range of size. Bryson and Bischoff argue that the key factor in asbestos carcinogenicity is the formation of a unique avascular fibrous tissue in response to chemically inert materials (*28*). These experiments do not challenge this argument, because the incidence of mesotheliomas correlated with the extent of fibrous tissue in the lesions. Of particular significance in examining particle structure in relation to carcinogenesis will be the testing of both glass and asbestos in narrow ranges of fiber size and totally reduced to nonfibrous form. Microfibers of other types of durable material, particularly those unrelated chemically to asbestos or glass, also must be tested.

REFERENCES

(*1*) WAGNER JC: Experimental production of mesothelial tumours of the pleura by implantation of dusts in laboratory animals. Nature (London) 196:180–181, 1962

(*2*) WAGNER JC, BERRY G: Mesotheliomas in rats following inoculation with asbestos. Brit J Cancer 23:567–581, 1969

(*3*) SMITH WE, MILLER L, ELSASSER RE, et al: Tests for carcinogenicity of asbestos. Ann NY Acad Sci 132: 456–488, 1965

(*4*) WAGNER JC: The induction of tumours by the intrapleural inoculations of various types of asbestos dust. *In* Lung Tumours in Animals (Severi L, ed.). Division of Cancer Res, Univ of Perugia, Perugia, Italy, 1966, pp 589–606

(*5*) WAGNER JC, BERRY G, TIMBRELL V: Mesotheliomas in rats following the intrapleural inoculation of asbestos. *In* Pneumoconiosis: Proceedings of the International Conference, Johannesburg, 1969 (Shapiro HA, ed.). New York, Oxford Univ Press, 1970, pp 216–219

(*6*) WAGNER JC: The pathogenesis of tumors following the intrapleural injection of asbestos and silica. *In* Morphology of Experimental Respiratory Carcinogenesis (Nettlesheim P, Hanna MG, Deatherage, JW, eds.). AEC Symposium Monograph Series #21. Oak Ridge, Tenn., Oak Ridge National Laboratory, 1970, pp 347–358

(*7*) STANTON MF, BLACKWELL R, MILLER E: Experimental pulmonary carcinogenesis with asbestos. Amer Industr Hyg Assoc J 30:236–244, 1969

(*8*) DONNA A: Tumori sperimentali da amianto di crisotilo, crocidolite e amosite in ratto Sprague-Dawley. Med Lavoro 61:1–32, 1970

(*9*) Report and recommendations of the working group on asbestos and cancer. Ann NY Acad Sci 132:706–721, 1965

(*10*) TIMBRELL V, GILSON JC, WEBSTER I: UICC standard reference samples of asbestos. Int J Cancer 3:406–408, 1968

(*11*) TIMBRELL V: Characteristics of the International Union Against Cancer standard reference samples of asbestos. *In* Pneumoconiosis: Proceedings of the International Conference, Johannesburg, 1969 (Shapiro HA, ed.). New York, Oxford Univ Press, 1970, pp 28–36

(*12*) Data sheets of physical and chemical properties of UICC standard reference asbestos samples. Circulated reports of The Dust Technologist. Pneumoconiosis Research Unit, P.O. Box 4788, Johannesburg, South Africa

(*13*) HARINGTON JS: Chemical studies of asbestos. Ann NY Acad Sci 132:31–47, 1965

(*14*) HARINGTON JS, ROE FJ: Studies of carcinogenesis of asbestos fibers and their natural oils. Ann NY Acad Sci 132:439–450, 1965

(*15*) TIMBRELL V, GRIFFITHS DM, POOLEY FD: Possible biological importance of fibre diameters of South African amphiboles. Nature (London) 232:55–56, 1971

(*16*) HUEPER WC: Experimental studies in metal cancerigenesis. I. Nickel cancers in rats. Texas Rep Biol Med 10:167–186, 1952

(*17*) BERRY G, WAGNER JC: The application of a mathematical model describing the times of occurrence of mesotheliomas in rats following inoculation with asbestos. Brit J Cancer 23:582–586, 1969

(*18*) MILLER LC, TAINTER ML: Estimate of the $E.D._{50}$ and its error by means of logarithmic probit graph paper. Proc Soc Exp Biol Med 57:862–864, 1944

(*19*) MAINLAND D, HERRERA L, SUTCLIFFE MI: Tables for Use With Binomial Samples. New York Univ, Dept of Med Statistics, 1956, p 79

(*20*) PILGRIM HI, DOWD JE: Correcting for extraneous death in the evaluation of morbidity or mortality from tumor. Cancer Res 23:45–48, 1963

(*21*) CHURG J, ROSEN SH, MOOLTEN S: Histological characteristics of mesothelioma associated with asbestos. Ann NY Acad Sci 132:614–622, 1965

(*22*) HARINGTON JS, GILSON JC, WAGNER JC: Asbestos and mesothelioma in man. Nature (London) 232: 54–55, 1971

(23) WAGNER JC: Asbestos cancers. J Nat Cancer Inst 46:5–9, 1971

(24) ROE FJ, CARTER RL, WALTERS MA, et al: The pathological effects of subcutaneous injections of asbestos fibres in mice: Migration of fibres to submesothelial tissues and induction of mesotheliomata. Int J Cancer 2:628–638, 1967

(25) WAGNER JC, SKIDMORE JW: Asbestos dust deposition and retention in rats. Ann NY Acad Sci 132:77–86, 1965

(26) CRALLEY LJ, KEENAN RG, LYNCH JR: Exposure to metals in the manufacture of asbestos textile products. Amer Industr Hyg Assoc J 28:452–461, 1967

(27) GROSS P, DETREVILLE RT, TOLKER EB, et al: Experimental asbestosis: The development of lung cancer in rats with pulmonary deposits of chrysotile asbestos dust. Arch Environ Health 15:343–355, 1967

(28) BRYSON G, BISCHOFF F: Silicate-induced neoplasms. Progr Exp Tumor Res 9:77–164, 1967

Figures 1-18

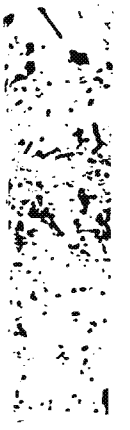

FIGURE 1.—South African crocidolite (Wagner preparation).

FIGURE 2.—Hand-milled crocidolite ore.

FIGURE 3.—Ball-milled crocidolite ore.

FIGURE 4.—UICC-SRAS crocidolite.

FIGURE 5.—UICC-SRAS amosite.

FIGURE 6.—UICC-SRAS chrysotile A.

FIGURE 7.—Partially pulverized UICC-SRAS crocidolite.

FIGURE 8.—Partially pulverized UICC-SRAS crocidolite.

FIGURE 9.—Partially pulverized AAA-coated glass.

STA

Figures 1–18.—Formvar suspensions of the 17 test materials arranged in order of carcinogenicity. × 261, except figure 8, × 4700

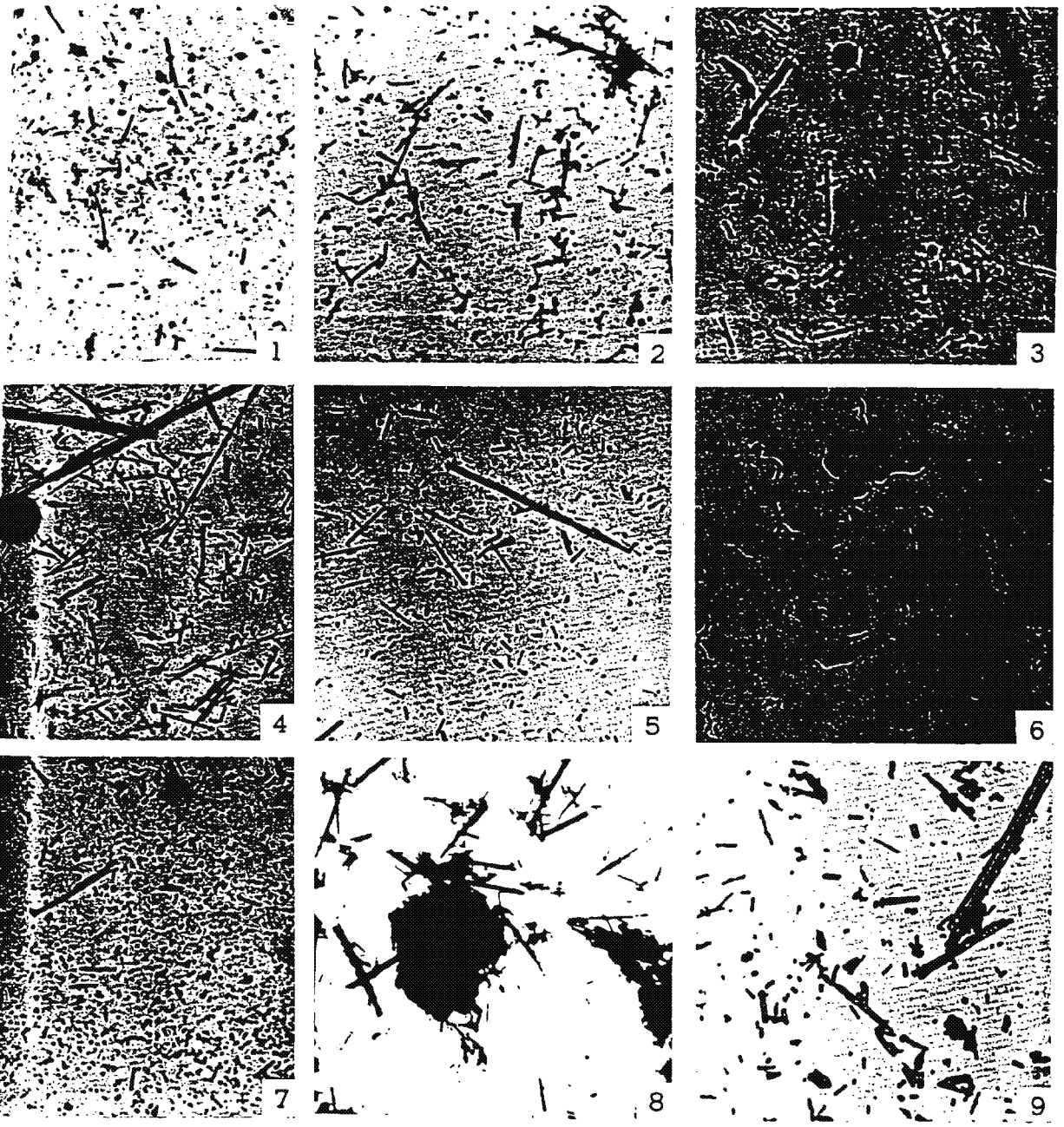

FIGURE 10.—Partially pulverized AAA-uncoated glass.

FIGURE 11.—Partially pulverized coarse glass vehicle.

FIGURE 12.—Cab-O-Sil, SiO_2.

FIGURE 13.—Partially pulverized Pyrex glass.

FIGURE 14.—Partially pulverized old glass wool.

FIGURE 15.—Silica soot, SiO_2.

FIGURE 16.—Whole coarse glass vehicle.

FIGURE 17.—Nickel metal fragments.

FIGURE 18.—Steel mill fragments.


10

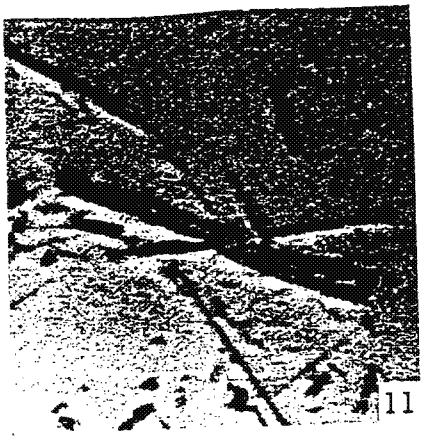
11

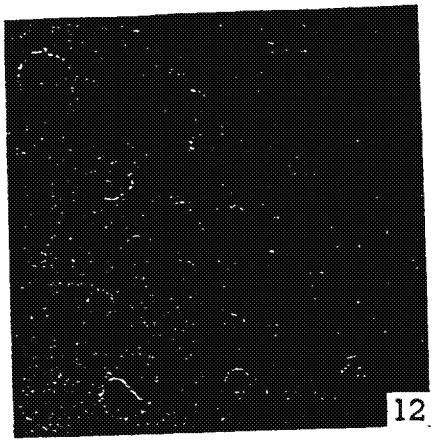
12

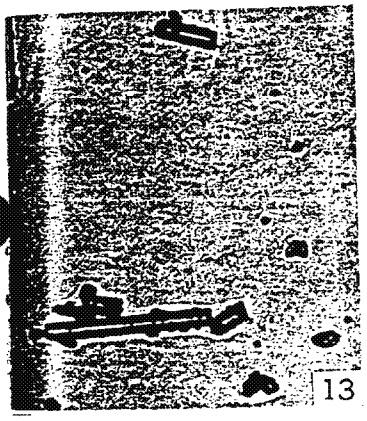
13

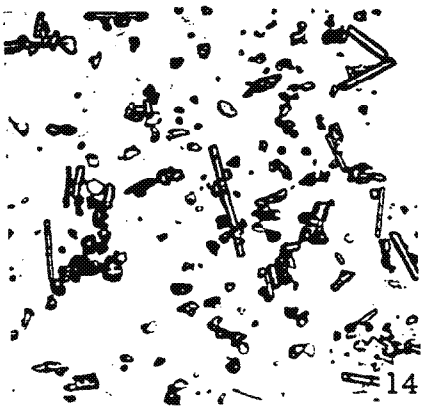
14

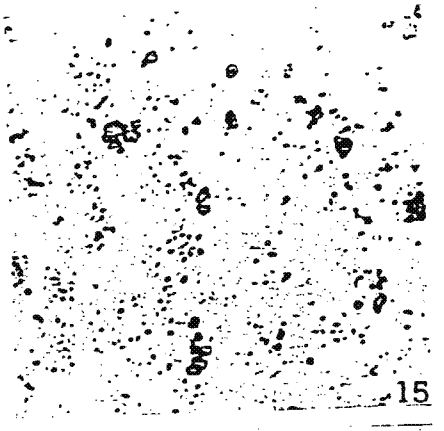
15

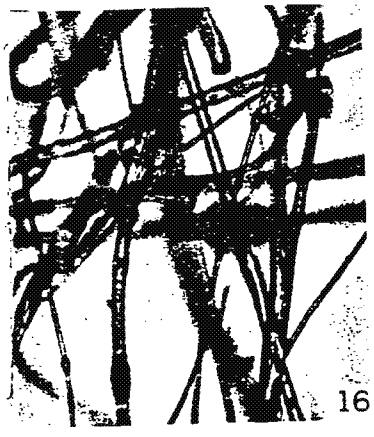
16

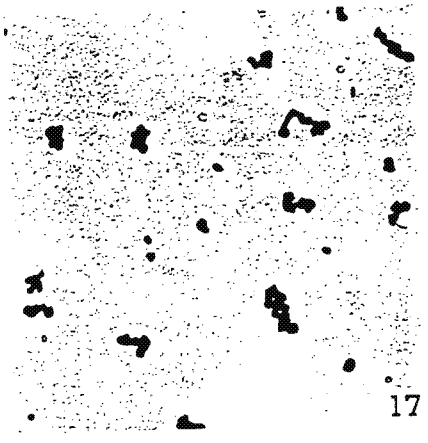
17

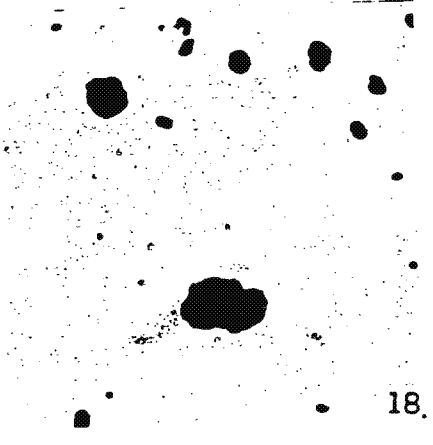
18

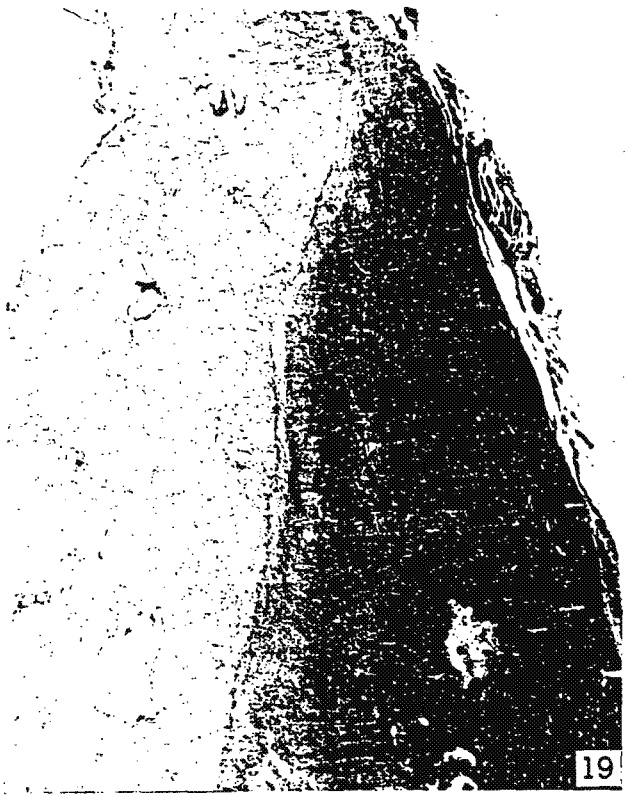

FIGURE 19.—Dense fibrous pleural plaque, typical of response to 40 mg UICC-SRAS asbestos. × 10

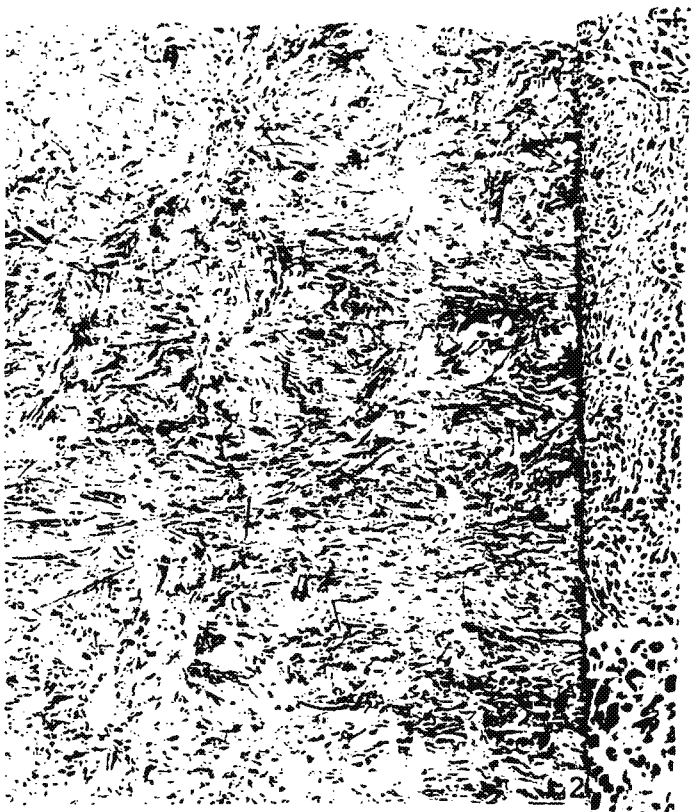

FIGURE 20.—Detail of dense fibrous pleural plaques induced by asbestos. *Note* abundant acellular collagen and crocidolite fibers. × 100

FIGURE 21.—Detail of pleural response to coarse fibrous glass vehicle infiltrated with nickel fragments. *Note* abundant vasculature and foreign body giant-cell reaction. × 100

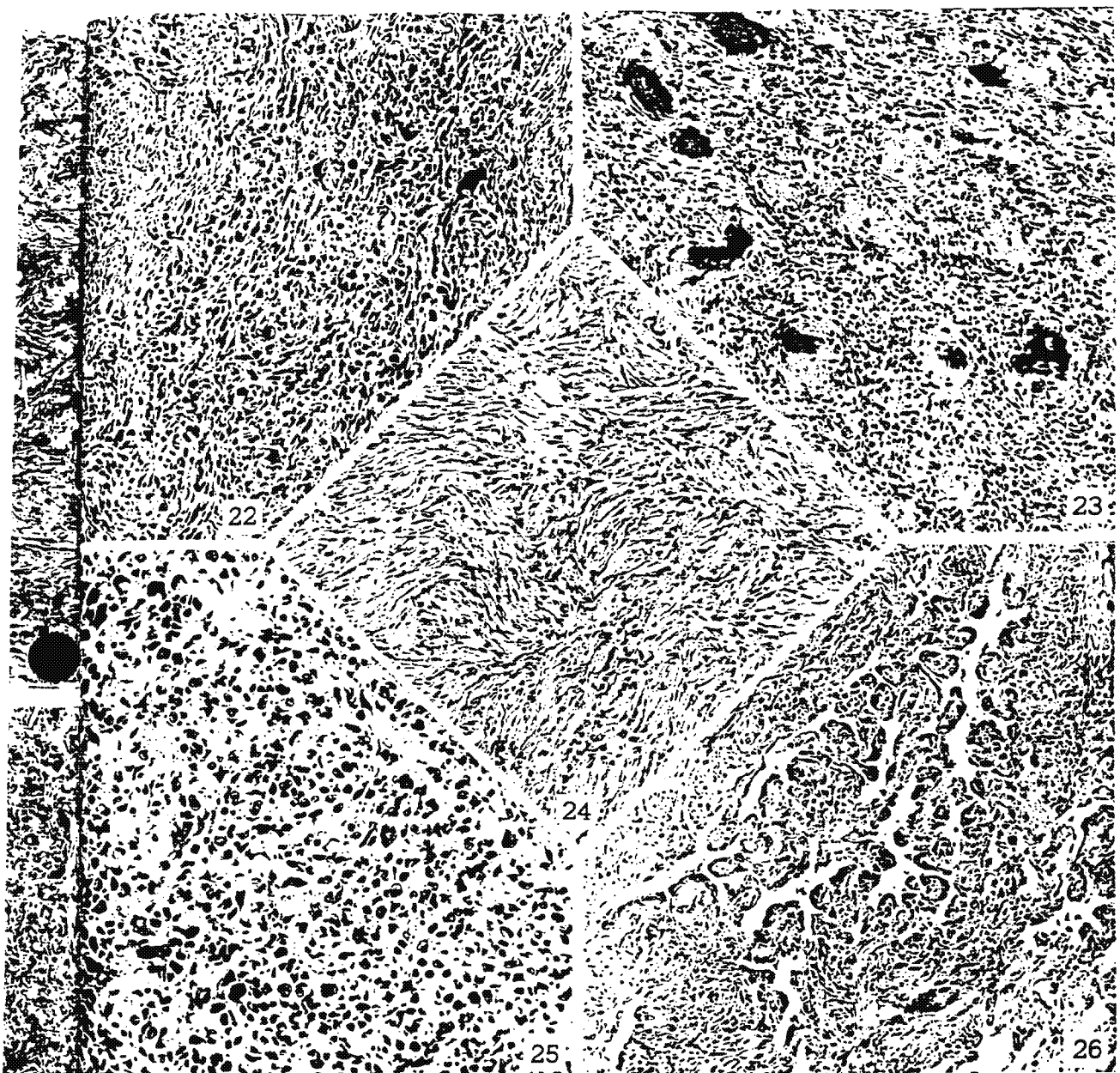

FIGURE 22.—Spindle-cell pleural mesothelioma with tumor giant cells. × 130

FIGURE 23.—Spindle-cell pleural mesothelioma with foci of osteogenesis. × 130

FIGURE 24.—Spindle-cell pleural mesothelioma with whorled and fasciculated pattern. × 130

FIGURE 25.—Pleomorphic pleural mesothelioma with medullary pattern. × 130

FIGURE 26.—Pleomorphic pleural mesothelioma with tubulopapillary pattern. × 130